Interactions at the Organic/Inorganic Interface: Molecular Modeling of the Interaction between Diphosphonates and the Surfaces of Barite Crystals

A. L. Rohl,[†] D. H. Gay,[†] R. J. Davey,[‡] and C. R. A. Catlow*,[†]

Contribution from The Royal Institution of Great Britain, 21 Albemarle Street, London W1X 4BS, UK, and Department of Chemical Engineering, UMIST, PO Box 88, Manchester M60 1QD, UK

Received May 3, 1995[⊗]

Abstract: Molecular modeling techniques are used to investigate the interaction of alkyldiphosphonate molecular anions with the surfaces of barium sulfate. We show that the most stable sites are on the (100) and (011) surfaces with the $[PO_3]^{2-}$ groups of the diphosphonates replacing surface sulfate ions. These results are compared with experimental observations; and analysis of the calculated energies demonstrates that the overall binding energy represents a subtle balance between the internal energy of the diphosphonate and the binding energy of the distorted diphosphonate in the site.

1. Introduction

Molecular recognition at the interface between inorganic materials and organic templates is known to be a powerful force in the control of crystallization and mineralization in both synthetic and biological systems. Thus, for example, the synthesis of micro- and mesoporous zeolites for adsorptive and catalytic applications depends very sensitively on the presence of single and assembled templating molecules.[1] Monolayers of appropriately functionalized amphiphilic monolayers are able to nucleate a range of inorganic materials[2] and in biological systems polysaccharidic and proteinaceous templates are responsible for skeletal development in a range of organisms.[3] Perhaps the simplest and best known example of this recognition process occurs during crystal growth in the presence of morphology modifying additives. In the past, morphological and structural data have been used to infer the essential elements of the interactions involved.[4,5] The control and inhibition of crystal growth is a major problem in several contemporary technologies. In many inorganic systems, the most efficacious growth modifiers are found to be polyanions, in which several charged groups are joined by a backbone. A particularly important case is provided by $BaSO_4$, whose precipitation in oil pipes is a significant problem in oil extraction and transport.[6] The most commonly used inhibitors for the growth of crystals of this compound are polyphosphonates of which the most widely studied are diphosphonates.[7,8] Growth inhibition of barite by these additives is thought to involve the incorporation of the inhibitor into a growing terrace, where it occupies the sites of two sulfate groups. Experimental evidence shows that diphosphonates are actually incorporated into the surface rather than just adsorbed onto the surface. In particular, it is found that similar dicarboxylates and disulfonates have no effect on crystallization.[8] The most obvious explanation of the latter is the mismatch between the single negative charge of the terminal groups and the double negative charge on the sulfate group. Moreover, Scanning Force Microscope experiments[9] have shown that if commercially available polyphosphonate growth inhibitors are added to growing calcite crystals, they appear on the images at step edges. Once the diphosphonate is in place, it blocks the crystal growth when a step edge reaches it. Indeed, Monte Carlo simulations[10] have shown that the presence of a single ion impurity is enough to block step growth. A large impurity that binds simultaneously at two surface sites will be much more efficient at blocking step growth than a single ion impurity.

The aim of this paper is to investigate at the molecular level the interaction between diphosphonate inhibitors and the surfaces of $BaSO_4$. Our approach is based on the use of computer modeling techniques which allow us to calculate directly the structures and energies of the relevant barite surfaces and of the growth inhibitor bound to them. These calculations provide considerable insight into the experimental observations on the effects of inhibitors on crystal growth. Analysis of the results, moreover, gives considerable insight into the complex interplay of the factors controlling the binding energy.

2. Methodology

1. Computational Method. We simulated the docking of propane-1,3-diphosphonate molecules onto barite surfaces using our new surface simulation code MARVIN,[11] which is particularly suitable for studying the interaction between molecules and inorganic surfaces containing molecular ions. The basic methodology (which is the same as in the earlier MIDAS code[12]) includes a two-dimensional Ewald sum[13] for

[†] The Royal Institution of Great Britain.

[‡] UMIST.

[⊗] Abstract published in *Advance ACS Abstracts,* December 15, 1995.

(1) Davis, M. E.; Lobo, R. F. *Chem. Mater.* **1992**, *4*, 756−768.

(2) Heywood, B. R.; Mann, S. *Langmuir* **1992**, *8*, 1492−1498.

(3) Weiner, S. *CRC Crit. Rev. Biochem.* **1986**, *20*, 365−408.

(4) Addadi, L.; Berkovitch-Yellin, Z.; Weissbuch, I.; Lahav, M.; Leiserowitz, L. *Top. Stereochem.* **1986**, *16*, 1−85.

(5) Davey, R. J.; Polywka, L. A.; Maginn, S. J. In *Advances in Industrial Crystallisation*; Garside, J., Davey, R. J., Jones, A. G., Eds.; Butterworth-Heinemann: Oxford, 1991; pp 150−165.

(6) Benton, W. J.; Collins, I. R.; Cooper, S. D.; Grimsey, I. M.; Parkinson, G. M.; Rodger, S. A. *Faraday Discuss.* **1993**, *95*, 281−297.

(7) Black, S. N.; Bromley, L. A.; Cottier, D.; Davey, R. J.; Dobbs, B.; Rout, J. E. *J. Chem. Soc., Faraday Trans.* **1991**, *87*, 3409−3414.

(8) Davey, R. J.; Black, S. N.; Bromley, L. A.; Cottier, D.; Rout, J. E. *Nature* **1991**, *353*, 549−550.

(9) Hillner, P. E.; Manne, S.; Hansma, P. K.; Gratz, A. J. *Faraday Discuss.* **1993**, *95*, 191−197.

(10) van Enckevort, W. J. P. In *Science and Technology of Crystal Growth*; van der Eerden, J. P., Bruinsma, O. S. L., Eds.; Kluwer: Dordrecht, 1995; pp 355−366.

(11) Gay, D. H.; Rohl, A. L. *J. Chem. Soc., Faraday Trans.* **1995**, *91*, 925−936.

(12) Tasker, P. W. *A guide to MIDAS*; AERE Harwell Report No. 9130, 1978.

0002-7863/96/1518-0642$12.00/0

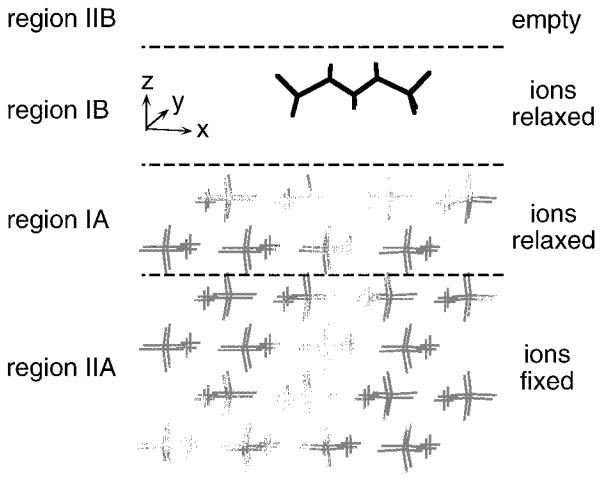

Figure 1. The MARVIN simulation cell used to dock a diphosphonate ion on a barite surface. The cell is repeated infinitely in the *x* and *y* directions. The region I atoms are allowed to relax while those in region II are kept fixed. The cell has been rotated slightly so that the two vacant sulfate sites can be seen. The size of the cell and the number of ions included in the surface regions has been greatly reduced for clarity.

treating the Coulomb interactions. However, the new code is far more effective in modeling crystals containing molecular ions as it prevents them from being cleaved during the surface generation process. Moreover, it is better adapted to model molecules on surfaces since this requires the inclusion of molecular mechanics potentials with the parameters being determined by connectivity rather than the distance criteria normally used in inorganic simulations.

The basic component in MARVIN is the simulation cell which has planar two-dimensional periodic boundary conditions parallel to the interface. The cell consists of one or more blocks, which are each split into two regions (I and II). Each region contains structural units, which may be ions or molecules consisting of one or more atoms. The atoms of the region I structural units are relaxed explicitly to zero force, while those in region II are kept fixed to reproduce the potential of the bulk lattice on region I. The total energy of the system is defined as the energy of all the region I structural units, which interact with each other, the region II structural units, and the periodic images of both regions. More details of the code are given in ref 11, which also demonstrates its accuracy and reliability for this type of calculation.

Thus in the present calculations the surface, as shown in Figure 1, consists of one block (A) with the structural units near the surface in its region I (designated region IA) and several planes further into the crystal in region II. The latter region is necessary to reproduce the electrostatic and short-range potential of the bulk lattice on region I. A molecule (or more accurately a periodic array of molecules) to be docked onto a surface is formally in region I of another block (B), while the corresponding region II of this block is empty.

2. Interatomic Potentials. Three sets of potentials are required to model the interaction of a diphosphonate ion with a barite surface. First, we must model the interactions within the barite crystal for which we use an ionic/molecular hybrid potential set which is discussed in detail in ref 14. Here, the sulfate ion is explicitly treated as a molecular system and atom···atom pair potentials describe the interactions between the sulfate species and the Ba^{2+} ions. These potentials are of two types—*inter* (Ba−O, O−O) and *intra* (S−O and O−S−O). Buckingham (or 6-exp) forms were used for the former, while for the latter, the interactions within the sulfate ion were described by a Morse potential acting between S and O and an O−S−O three-body term. Second, we model interactions within the diphosphonate anion using the molecular mechanics CVFF forcefield available in the Biosym Discover code[15] in which atomic charges are determined from the Mulliken population analysis obtained from the PM3 semiempirical quantum mechanical technique in the MOPAC package.[16] The charge distributions were also calculated using the MNDO and AM1 techniques also in the MOPAC package with similar results. The potentials between the surface and the anion were obtained from three sources. First, the forces between oxygen atoms of the anion were assumed to be the same as those in barite and so the O−O interaction from the barite potential set was used. Second, the interactions between the oxygen ions at the surface and the rest of the diphosphonate were taken from the CVFF forcefield. Third, the corresponding barium potentials are from the UFF forcefield of Rappé and co-workers.[17] Clearly it would be desirable to have forcefields developed specifically for describing the diphosphonate−surface interaction, the most promising source for which would be detailed *ab initio* calculations. Since, however, the interactions are dominated by electrostatic and steric factors, the present parametrization is adequate for the purpose of this study.

3. Docking Procedure. We recall that the docking of the diphosphonate involves the *replacement* of surface sulfates. Thus to determine which crystal faces will be affected by an additive, we must calculate the energetics of the process in which two surface sulfate ions are replaced by the additive. First, however, the surface structure of each growing face must be investigated. In general, faces corresponding to a given Miller index may have several different surface structures in which the crystal is cleaved in different places.[18] In barite, only the (010) face has a unique surface structure. For all the other faces considered, we calculated for each possible structure both the attachment energy (the energy per molecule released when a new slice of depth d_{hkl} is attached to the growing crystal face) and the surface energy (the difference in energy of the surface ions compared to those in the bulk per unit surface area). If the crystal growth is controlled by thermodynamic factors then the cut with the lowest surface energy will be dominant in the growing surface. If, on the other hand, the growth is kinetically controlled, the cut with the lowest absolute attachment energy will be most favored, as discussed in further detail in ref 11. For the faces of barite that we have considered (which are those appearing in the successful model of the barite morphology in ref 14), the surface cut with the lowest surface and absolute attachment energies were the same, leading to an unambiguous surface configuration for each face, except for the (100) which has two possible cuts which have very similar unrelaxed attachment energies of −303 kJ/mol. The difference between the two surface structures can be clearly seen by comparing Figure 3a (cut *a*) to Figure 7a (cut *b*). The top layer of the surface in the former is a sulfate layer whereas for the latter it is a layer of barium atoms. The surface in Figure 7a can be simply generated from Figure 3a by removing the top sulfate and barium layer in the latter. Thus calculations have been performed on both configurations of this face. Note, however, that allowing the surface to relax produces a significant difference in the attachment energies (−274 kJ/mol vs −248 kJ/mol). Given the high quality of the potentials for $BaSO_4$, this difference is significant, suggesting that perhaps cut b will be the favored surface configuration.

For each surface, there are many combinations of pairs of sulfates which can be replaced by a diphosphonate as discussed in greater detail below. Since the P−P distance in the solution conformation of diphosphonate determined by MOPAC calculations is 6.17 Å, it seems reasonable to exclude those pairs of sulfates with a S−S distance greater than 7.5 Å, which results in six possible unrelaxed S−S distances (4.02, 4.52, 5.25, 5.47, 5.66, and 7.06 Å) although the list becomes more extensive after relaxation. In the first set of calculations, we used a simulation cell which was a 2 × 2 supercell of the surface of barite which was large enough to contain all S−S pairs less than 7.5 Å apart. For each pair of sulfates removed, a diphosphonate was inserted into the vacated area and both the surface ions and diphosphonate were allowed to relax to minimize the total energy.

The most physically significant term is the *replacement energy* ΔE_{repl}, *i.e.* the energy change on replacement of two sulfates in a surface with

(13) Heyes, D. M.; Barber, M.; Clarke, J. H. R. *J. Chem. Soc., Faraday Trans. 2* **1977**, *73*, 1485−1496.

(14) Allan, N. L.; Rohl, A. L.; Gay, D. H.; Catlow, C. R. A.; Davey, R. J.; Mackrodt, W. C. *J. Chem. Soc., Faraday Discuss.* **1993**, *95*, 273−280.

(15) InsightII Version 2.3.6, Biosym Technologies Inc.: San Diego, 1995.

(16) MOPAC Version 5.0, QCPE No 455, Department of Chemistry, Indiana University, 1989.

(17) Rappé, A. K.; Casewit, C. J.; Colwell, K. S.; Goddard, W. A., III; Skiff, W. M. *J. Am. Chem. Soc.* **1992**, *114*, 10024−10035.

(18) Hartman, P.; Strom, C. S. *J. Cryst. Growth* **1989**, *97*, 502−512.

Table 1 The Most Favorable Replacement Energies Calculated for the Different Faces of Barite[a]

face	S−S (Å)	S−S$_{rel}$ (Å)	P−P (Å)	ΔE_{repl} (kJ/mol)	E_{diphos} (kJ/mol)
(100)*s*	5.47	5.47	5.31	−303	1075
(011)	5.66	5.77	5.10	−298	878
(010)	4.52	4.63	4.08	−231	1134
(001)	5.47	5.47	4.91	−218	1048
(100)*b*	4.02	4.32	4.35	−189	1024
(210)	4.02	4.39	4.01	−188	1075
(211)	5.25	5.09	4.50	−184	1049
(101)	5.47	5.47	4.82	−148	1087

[a] The sulfur−sulfur distances indicate which pair of sulfates have been removed from the surface, the first referring to the unrelaxed surface and the second to the relaxed. The phosphorus−phosphorus distance is for the final configuration of the docked diphosphonate in the surface.

a diphosphonate ion. This can be calculated as follows:

$$\Delta E_{repl} = (E_{surf} + E_{diphos} + E^{solv}_{diphos}) - (E_{surf+diphos} + 2E_{sulf} + 2E^{solv}_{sulf})$$

where E_{surf} is the total energy of the system containing just the relaxed surface; $E_{surf+diphos}$ is the total energy of the system without two sulfates but with the docked diphosphonate; E_{diphos} is the internal energy of the isolated minimized diphosphonate ion (640 kJ/mol); E_{sulf} is the energy of the isolated minimized sulfate ion (−1,930 kJ/mol), and E^{solv}_{diphos} and E^{solv}_{sulf} are the solvation energies of the diphosphonate (−2,734 kJ/mol) and sulfate (−1,019 kJ/mol), respectively. The solvation energies are calculated by inserting the target ion into a sphere of water with a radius of 15 Å and performing 350 steps of molecular dynamics at 270 K, followed by minimization, resulting in an energy for the ion surrounded by its hydration sheath ($E_{water+ion}$). The target ion is then removed and the same steps performed on the sphere of water only, yielding the energy of the hydration sheath (E_{water}). The solvation energies are then calculated by the expression:

$$\Delta E^{solv}_{ion} = E_{water+ion} - (E_{water} + E_{ion})$$

where E_{ion} is the internal energy of the isolated ion. The procedure was repeated five times and the average value of ΔE^{solv}_{ion} calculated. Despite the simplicity of this approach, it may be expected to yield a reasonable estimate of the hydration energy.

We note that the use of the replacement energy does not imply that the mechanism of incorporation involves the inhibitor replacing two sulfate anions from the perfect surface. Rather it allows us to assess the thermodynamic stability of the docked diphosphonate anions.

Returning to the simulation of the docking of a diphosphonate onto the barite surface, we attempted to locate the global minimum for each surface. This was done for each face/site combination by placing the inhibitor in many different starting positions. For a given combination, the minimum was found to be independent of the starting position in the majority of cases. For the others, different minima were found but the difference in the energy between the top three or four (∼30 kJ/mol) was found to be smaller than the differences between the most favorable replacement energies for the different faces. In the final set of calculations, for which detailed results are reported here, the most energetically favorable configurations from each 2 × 2 surface were embedded in a 4 × 4 surface and the whole ensemble relaxed. The energies obtained from these larger cells should have only small contributions from interactions between diphosphonates in neighboring cells.

Finally, regarding the errors in the calculated energies, those associated with computational and numerical aspects (*e.g.* cutoffs in summations) are low and would be expected to lead to errors of <1 kJ/mol in the calculated values of ΔE_{repl}. It is difficult to quantify precisely the uncertainties associated with the interatomic potentials. We consider, however, that these will not influence the main conclusions drawn from our results. Thus if we refer to the results in Table 1, which are discussed in detail below, the calculated differences between the ΔE_{repl} for the (011) and (010) surfaces are certainly of significance, while those between (100)*a* and (011) surfaces are probably within the uncertainties due to the approximations made in the potential models.

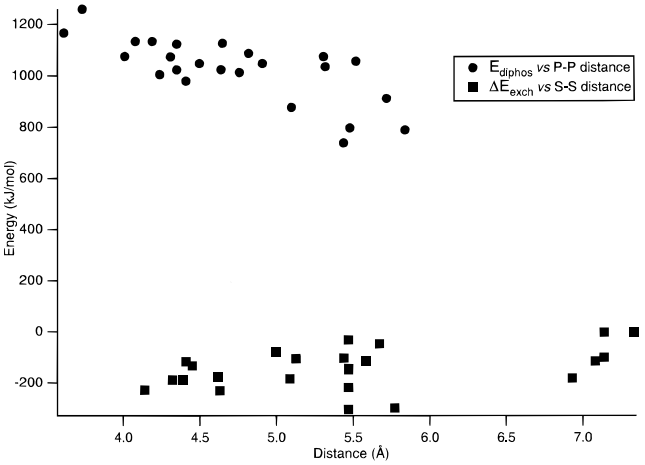

Figure 2. The internal energies of the docked diphosphonate ions vs their P−P distances (solid circles) and the replacement energies for replacing two surface sulfates with a diphosphonate vs the relaxed S−S distances of the two sulfates (solid squares).

3. Results and Discussion

The results for the most favorable replacement energy for each face considered in this study are summarized in Table 1. They show that the diphosphonate anions will bind preferentially to *two* faces: (011) and the *a* cut of (100). There is then an energy difference of almost 70 kJ/mol until the next closest replacement energy which occurs at the (010) face.

The factors controlling the structure and stabilities of the docked inhibitor are clearly complex. But can we understand in qualitative terms the factors controlling the replacement energy? There are two main contributions to this term: first, the *internal energy* of the diphosphonate which increases as the ion is distorted to fit into the docking site, and second, the *binding energy* of the distorted diphosphonate in the site; the latter in turn depends on the stereochemical match between the docked diphosphonate oxygen atoms and the vacant oxygen sites at the surface. Further factors will be the extent of distortion of the lattice ions surrounding the docked molecule and the magnitude of the interactions between the diphosphonate backbone and the surface. In the section which follows we consider these items in detail; but first we must review the sites available for the docked inhibitor.

1. Docking Sites. A key feature of the docked structure is the *separation* between the replaced sulfate groups; indeed, in the future we refer to docking sites by the distance between the vacant sulfate pairs in the unrelaxed surface. For the (100)*a* and (011) faces, the most stable docking site has the sulfate pairs separated by 5.47 and 5.66 Å, respectively, which is close to the ideal diphosphonate P−P distance of 6.20 Å. But this behavior is not observed for all faces; for example, in (210) the 4.02 Å site is ∼90 kJ/mol more stable than the 5.25 and 5.66 Å sites. This point is emphasized in Figure 2, which shows the variations with sulfate group separation of the replacement energy for all configurations calculated in the 4 × 4 simulation cells. It is clear that there is no direct correspondence between these quantities. Thus with the exception of the two most stable docking sites, the figure shows that docking into sites with relaxed distances between 4.39 and 4.63 Å ("small sites") results in structures that are as stable if not more stable than their counterparts at distances from 5.00 to 5.67 Å ("medium sites"). The stabilities of diphosphonates in sites greater than 6.93 Å ("large sites") are on average significantly less, and for none

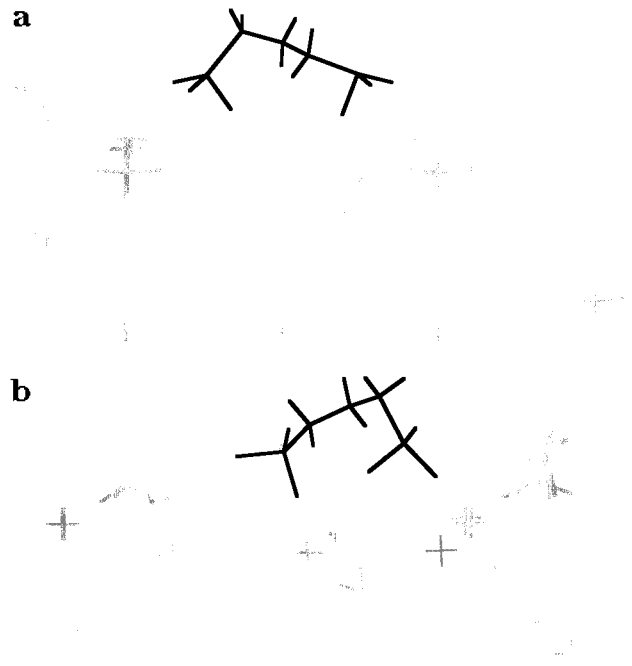

Figure 3. The two most stable docking sites for an alkyldiphosphonate on the surfaces of barite (a) on the 5.47 Å site on the a cut of the (100) surface and (b) on the 5.66 Å site on the (011) surface. The diphosphonate is colored black and the surface barite ions gray.

of the faces considered is any of these the most stable site, as shown from the results in Table 1.

The reasons for this complex variation of the replacement energy will become clearer when we examine the component energy terms.

2. Internal Energies. First let us examine the internal energy as a function of the P−P distance of the docked diphosphonate which is also shown in Figure 2. The most striking aspect of these results is that they show that the diphosphonate ion cannot attain P−P distances as large as the S−S separation of the large sites. In fact the largest P−P distance calculated is 5.84 Å, which is significantly shorter than the 6.20 Å attained in the solution configuration. The explanation is simple: the hydrogen atoms on the central carbon atom of the diphosphonate in the solution configuration are below the phosphorus atoms and will interfere with the barite surface when docked forcing the ion to distort, resulting in a smaller P−P distance. Figure 2 also shows that the internal energy of the diphosphonate decreases with increasing P−P distance as expected; but the spread in internal energies for medium distances is large compared to that for the small distances. A simple approach might suggest that the variation in replacement energy simply reflects the dependence of the internal energy of the diphosphonate ion on the P−P distance. However, the internal energies listed in Table 1 provide a clear refutation of such a model, as although the (011) configuration has a low internal energy, that for the (100)*a* configuration is almost 200 kJ/mol larger; nevertheless, the two configurations have similar replacement energies.

To understand the origins of these variations in internal energies, we now explore the structures of the docked diphosphonate ions in greater detail. Figure 3 shows their configurations in the two most stable sites. Both diphosphonate configurations have similar backbone structures and the internal energies, *omitting terms arising from the oxygen atoms*, are 187 kJ/mol for docking into the (100)*a* site and 210 kJ/mol for the (011) site. But we recall from Table 1 that the total internal energy of the latter is almost 200 kJ/mol lower than that for

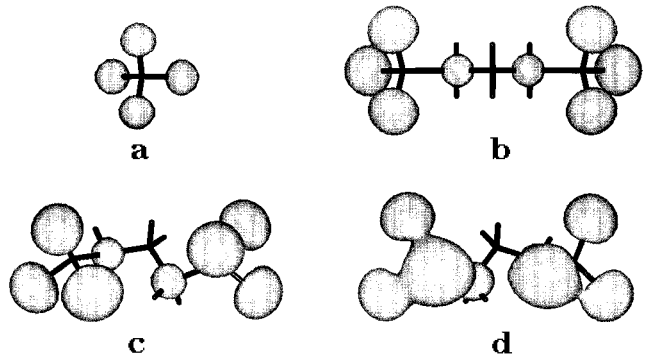

Figure 4. Electrostatic potential surfaces corresponding to −2100 kJ/mol (gray) (a) for a sulfate ion, (b) for the equilibrium configuration of diphosphonate, and (c, d) for the two configurations of the diphosphonates that lead to the lowest exchange energies on the (011) and (100) surfaces, respectively.

the former, which must therefore be attributable to interactions involving the O atoms. There are two distinct causes of this difference. In the (100)*a* diphosphonate, the two diphosphonate groups are eclipsed, resulting in a large Coulombic repulsion between two of the O atoms; for the (011) case, they are staggered and thus the Coulombic repulsion is smaller. We can see this effect clearly in Figure 4, where the electrostatic potential is contoured at −2100 kJ/mol for the sulfate and diphosphonate configurations appropriate for the solution and for adsorption of the latter in the (100)*a* and (011) surfaces. For the diphosphonate molecules, the view is from beneath showing the potential as presented to the barite surface. The relative orientation of the phosphonates at each end of the diphosphonate ion is determined by the barite surface as the phosphonate groups bind most effectively to the vacant sulfate sites. In (100)*a*, the two vacant sulfates are related by a mirror plane and thus the two phosphonates are arranged with an approximate mirror plane through the center of the diphosphonate ion. In (011), the vacant sulfates are related by only a translation which is reflected by the arrangement of the O atoms on the diphosphonate ion. Figure 4 also illustrates the second contribution to the internal energy which arises from the fact that in the (100)*a* configuration the O−P−O and C−P−O bond angles are much more distorted from their equilibrium values than for the (011) configuration.

3. Diphosphonate−Surface Binding Energy. It should now be clear that this second contribution to the replacement energy is at least as important as the first. In particular, the stability of the diphosphonate in the (100)*a* site must be due to a very favorable ion−surface interaction. The interactions between the ion and surface can be calculated first for the short-range interatomic potentials for which we find 384 kJ/mol for the (100)*a* site and 346 kJ/mol for the (011) site. The structures shown in Figure 3 clearly rationalize the difference: they show that the diphosphonate in (100)*a* is further away from the surface than is the case for the (011) surface. This energy difference is, however, far too small to outweigh the 200 kJ/mol difference in the internal energies of the two diphosphonates. Hence the determining factor must be the electrostatic interaction between the diphosphonate and surface ions. Of critical importance is the greater negative charge on the oxygen atom (−1.08) in the phosphonate group compared with those in the sulfate group (−0.84). The resulting large effect on the electrostatic potential is apparent in Figure 4, where the −2100 kJ/mol contour surfaces on the oxygen atoms in a sulfate ion are much smaller than their counterparts in a diphosphonate ion.

With these factors in mind let us now look at the local environment of the phosphonate groups. Figures 5 and 6 display

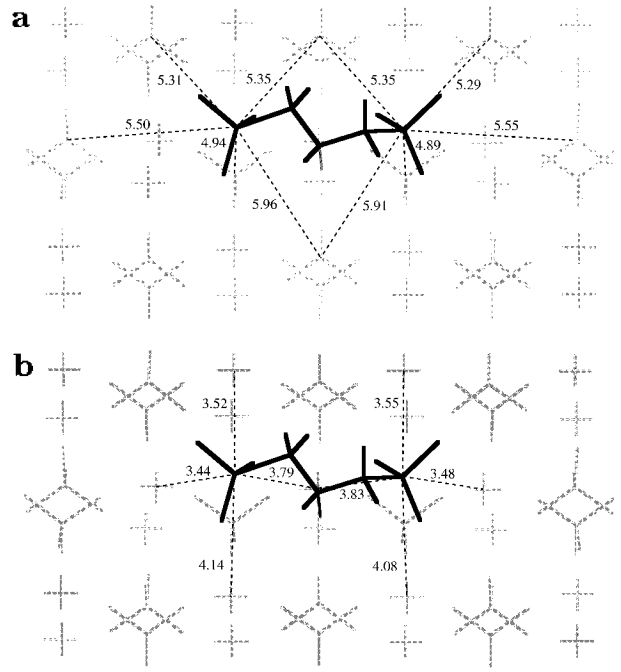

Figure 5. (a) P−Ba and (b) P−S distance between the docked diphosphonate and the surface ions in the 5.47 Å site on the barite (100)*a* surface.

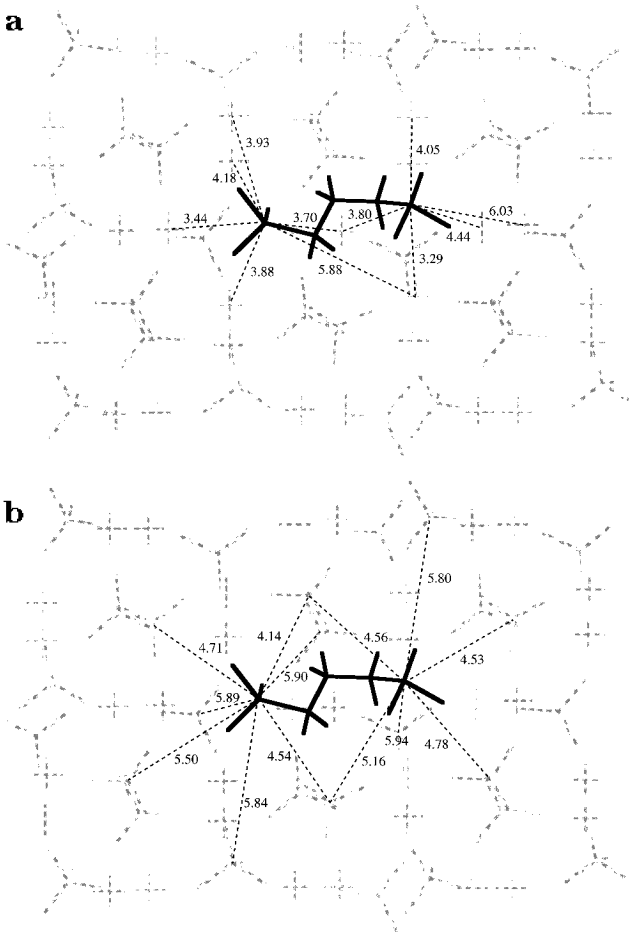

Figure 6. (a) P−Ba and (b) P−S distance between the docked diphosphonate and the surface ions in the 5.66 Å site on the barite (011) surface.

the phosphonate−sulfate and phosphonate−barium distances that are less than 6.0 Å for adsorption on (100)*a* and (011), respectively. Looking first at the configuration on (100)*a*, each

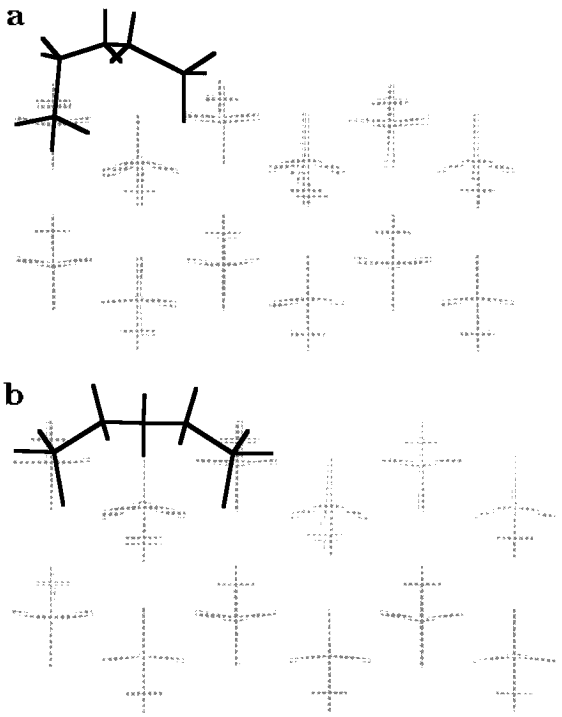

Figure 7. Two of the minima found for docking a diphosphonate into the 5.47 Å site on cut *b* of the (100) surface.

phosphonate group is close to five sulfates, with only one closer than 5.0 Å, and the rest being at distances between 5.31 and 5.96 Å. In contrast for adsorption on (011), one phosphonate has seven sulfate neighbors, while the other has six, and in both cases three of them are closer than 5.0 Å. Clearly the diphosphonate on (011) will be more strongly repelled by its neighboring sulfates than that on (100)*a*. At the same time, the diphosphonate is attracted to its nearest neighbor barium ions. Each phosphonate on (100)*a* has four neighboring barium ions with three of them closer than 4.0 Å. In (011), one phosphonate has six barium neighbors and the other five, with the former having four closer than 4.0 Å, and the latter, two. The change in the interaction with the cation is not, however, sufficient to outweigh the effect of the repulsive interaction with the very close sulfate neighbors and thus the diphosphonate in the (100)*a* site has a stronger ion−surface interaction than that in the (011) site.

The other surface which has a large number of close sulfate−sulfate distances is the second cut of the (100) surface—(100)*b*; and we see dramatic effects when docking a diphosphonate onto this surface with two vacant sulfates separated by 5.47 Å. The replacement energy for this site is −143 kJ/mol and the final configuration of the surface and diphosphonate is illustrated in Figure 7a which shows that, surprisingly, one of the phosphonate groups is not docked fully into the surface. Figure 7b shows one of the other minima found in the investigation of this site in which the diphosphonate is fully docked and the positions of the O atoms all match well those of the vacant sulfates. However, this configuration is about 10 kJ/mol *higher* in energy. The internal energy of the former diphosphonate is 979 kJ/mol and the latter is 790 kJ/mol, *i.e.* a difference similar to that between (001)*a* and (011). However, placing both phosphonates into the surface greatly disturbs the diphosphonate−surface Coulomb interaction and again produces a configuration which is overall slightly less stable than the one with the high internal energy.

The crucial role of the electrostatic interactions between the inhibitor and surface is apparent in other configurations with

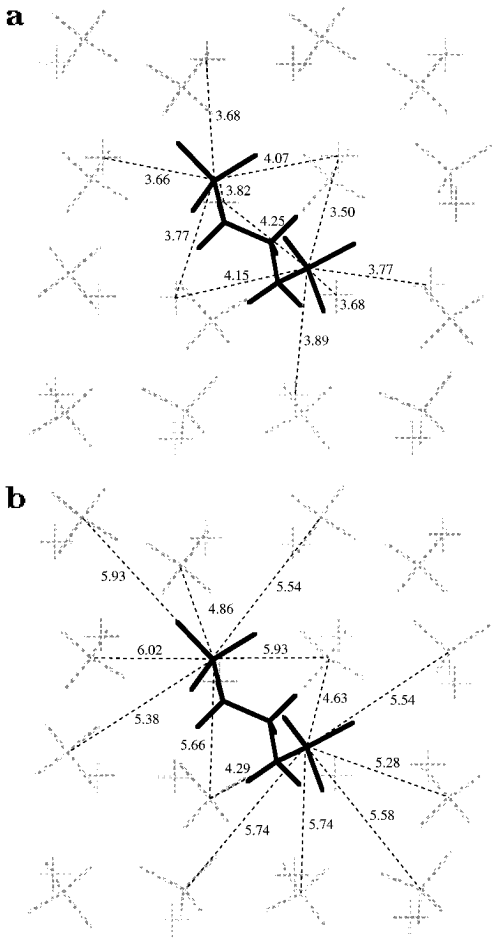

Figure 8. (a) P−Ba and (b) P−S distance between the docked diphosphonate and the surface ions in the 4.02 Å vacancy on the barite (210) surface.

short sulfate−sulfate distances. The results in Table 1 show that for some faces a diphosphonate in the 4.02 Å site is the most stable configuration. For the docked configuration in the (210) surface, we can rationalize this behavior by again looking at the nearest neighbor barium and sulfate distances to the diphosphonate ion. Figure 8 shows the phosphonate−sulfate and phosphonate−barium distances that are closer than 6.0 Å to the diphosphonate docked in the 4.02 Å site in the (210) surface. Both phosphonate groups have seven neighboring sulfates with one having only one sulfate closer than 5.0 Å, and the other, two. The former group has five barium neighbors while the latter has six with both groups having four barium ions closer than 4.0 Å. Thus the diphosphonate in this site has more close neighboring barium ions than that docked in the (011) face and the sulfate neighbors are further away; *i.e.* omitting internal energies, the binding energy of the diphosphonate ion to the (210) surface is greater than that to the (011) surface. The (210) surface has four distinct sites for a diphosphonate ion, all with a similar distribution of neighboring sulfate and barium ions to that discussed above for the 4.02 Å site; the three other sites have unrelaxed S−S distances of 5.66, 5.66, and 5.25 Å. In Figure 9, the relaxed configurations of the diphosphonate and the (210) surface are overlaid for the 4.02 and 5.25 Å cases. The overlay is useful because it also shows the approximate position and orientation of the vacant sulfate groups that are being occupied by phosphonate groups. The figure shows that the relative orientations of the sulfate pairs of the two sites are very similar, the only significant difference being the separation between them. The oxygen atoms of the two phosphonate groups in the 4.02 Å site match

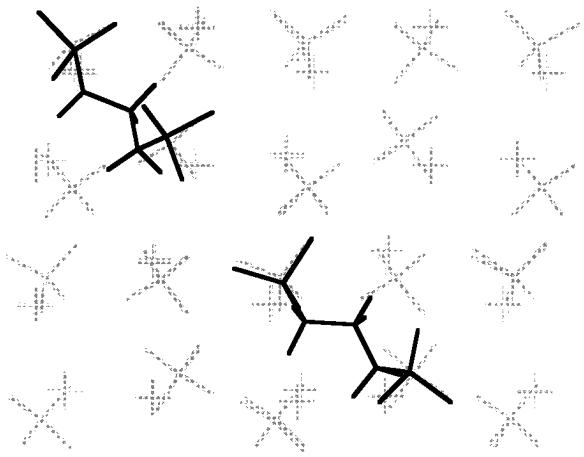

Figure 9. An overlay of the final diphosphonate and surface configurations for the 4.02 and 5.25 Å sites on the (210) surface.

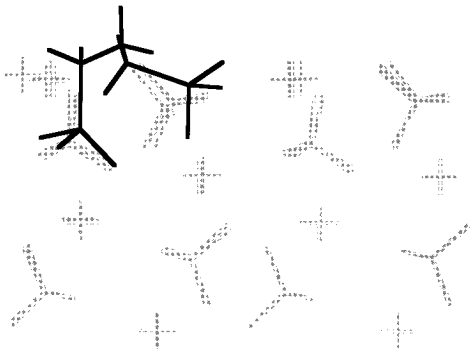

Figure 10. The relaxed diphosphonate and surface positions after docking a diphosphonate into the 4.02 Å site on cut *b* of the (100) surface.

the positions of the oxygen atoms of the sulfates more closely than they do in the case of the 5.25 Å site, the primary reason for which is that for a good correspondence between the oxygen positions of the vacant sulfate and phosphonate group, the carbon atom which connects the phosphonate to the backbone needs to occupy a site near the fourth oxygen atom of the vacant sulfate group, as is clearly achieved for the diphosphonate ion in the 4.02 Å site but not for the diphosphonate ion in the 5.25 Å site. The inability of the latter diphosphonate ion to match fully the vacant sulfate positions is a direct result of the distance between them being close to the maximum attainable P−P distance which results in a strong constraint on the diphosphonate. Similar arguments hold for the two 5.66 Å sites. If the backbone connecting the two phosphonate groups was longer, presumably the three larger sites would become more stable than the 4.02 Å site.

The (100)*b* face discussed earlier also has the highest binding for a diphosphonate in a 4.02 Å site. It was found that on this face the diphosphonate will not match closely the vacant sulfate groups due to the presence of close sulfate neighbors which strongly repel the phosphonate groups. Indeed, the diphosphonate occupying this site is found to match the vacant oxygen sites badly as shown in Figure 10. The poorness of this fit is also reflected in the final P−P distance in the diphosphonate ion as it is the only one in Table 1 which is larger than that of the S−S distance of the vacant site. All other docked diphosphonates have shorter distances since the equilibrium P−O bond length (1.61 Å) is longer than that of the S−O bond (1.51 Å).

4. Adsorption Sites: Summary. The calculations presented here show that a subtle interplay of interactions determines the adsorption sites of a molecular ion into an inorganic surface. In particular, for a system with more than one attaching group,

these factors include the internal energy of the docking ion as it distorts to fit the surface, the extent to which the docking groups mimic the surface groups they replace, and the interactions of the backbone of the adsorbate with the surface. Note that this is a function of not only the adsorbing ion but also the individual surface structures. We should emphasize that the balance of these competing contributions to the replacement energy cannot be evaluated by a simple visual inspection of the adsorbing molecular ion and possible surface docking sites; they must be calculated explicitly, as in this study.

In the diphosphonate/barite system considered in this work, it has been shown that for some surfaces the phosphonate groups can match stereochemically the sulfate sites very closely which lead to the most stable configurations at that surface. For other faces, where the sulfate groups surrounding the docking sites are closer than average and the barium ions are further away, exact matching of the sulfate positions is not the most effective way to bind as the increased negative charge on the phosphonate groups relative to sulfate ions leads to increased repulsion. The two most stable sites for diphosphonate ions in the barite surface, which are very close in energy, each fall into one of these categories. For the (100)*a* surface, the diphosphonate preferentially binds into the 5.47 Å site by fitting the vacant sulfate positions well. In contrast, the diphosphonate preferentially binds to the (011) surface in the 5.77 Å site but does not match the sulfate positions well. However, it has a very small internal energy, which compensates for the relatively poor fit.

5. Comparison with Experiment. Experimentally the effects of diphosphonates on the crystallization of barite have been studied in some detail by Davey *et al.*[7,8,19] and Heywood and Mann.[2,20] The former studies dealt specifically with the effect of dissolved diphosphonates, of the type modeled here, on the crystal morphology, while the latter investigated the orientational relationship occurring during nucleation of barite under monolayers of alkylphosphonates and sulfates. For solution grown crystals, it was observed that additives such as amino dimethylene- and propane-1,3-diphosphonic acids induce the expression of {011} faces at low concentrations and attack the [001] zone of faces at higher concentration. This latter effect is maximized in the {010} direction with no effect seen in {100}. However, when nucleation takes place beneath monolayers, the surface in contact with the monolayer is always {100}. In comparing these data with the results of the calculations performed in the present study two factors must be considered. Firstly, favorable values for ΔE_{repl} do not necessarily imply that a surface will appear in the final morphology of the crystal since for this to happen the growth rate of the surface relative to other surfaces must also change.[19] Thus, for example, the appearance of the {011} faces observed by Davey *et al.*[7] is totally consistent with our calculations as is their definition of the binding site. However, the current prediction that these diphosphonates will also enter the {100} surface is not confirmed with an appropriate morphological change. Possibly the relative growth rates of the {100} and {210} faces remain essentially unchanged despite additive binding. However, the explanation is more likely related to the predicted efficacy of additive binding to {100}, namely the choice of growth slice, (100)*a* or *b*. As mentioned earlier, the magnitude of the *relaxed* attachment energy of (100)*b* is smaller than (100)a, *i.e*. the relaxed *b* slice is the slower growing and hence more stable surface structure. This is hardly surprising since visual observation of the surface structures shows that the *a* slice is the less close packed of the two. Interestingly this conclusion is entirely consistent with the results of the monolayer experiments in which the hexagonal array of phosphonate groups effectively simulates an *a* face with the nucleated surface a {100}*b* face. In relation to our results such an assignment would lead to agreement with the data of Davey *et al*. since as seen from Table 1 binding to the {100}*b* surface is energetically less favorable than to {010}.

Overall, therefore, agreement between the current modeling and experimental data is good with the surprising result that such comparison can aid discrimination between alternative surface structures.

4. Conclusions

The simulations described in this paper highlight the complexity of the processes controlling the interaction of flexible growth inhibiting molecules with crystal surfaces. In particular, molecular design of growth inhibitors cannot be solely based on geometric criteria, as shown by the stabilities calculated for "small sites", which would not be predicted as stable by such simple graphical methods. However, calculations of the type described here allow a detailed and accurate treatment of the competing terms controlling the inhibitor−surface interaction and will provide an increasingly powerful tool for the design of improved growth inhibitors.

Acknowledgment. We would like to thank the S.E.R.C., I.C.I., and Biosym Technologies for their financial support. We are indebted to Biosym Technologies, San Diego for supplying the InsightII code used for the graphical representations in this study.

Supporting Information Available: A listing of the potential parameters used in this study (3 pages). This material is contained in many libraries on microfiche, immediately follows this article in the microfilm version of the journal, can be ordered from the ACS, and can be downloaded from the Internet; see any current masthead page for ordering information and Internet access instructions.

JA951443J

(19) Bromley, L. A.; Cottier, D.; Davey, R. J.; Dobbs, B.; Smith, S.; Heywood, B. R. *Langmuir* **1993**, *9*, 3594−3599.

(20) Heywood, B. R.; Mann, S. *J. Am. Chem. Soc.* **1992**, *114*, 4681−4686.